Supporting Information

Maywald et al. 10.1073/pnas.1422445112

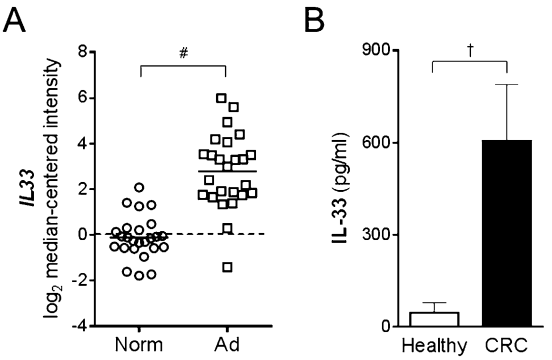

Fig. S1. IL-33 signaling associates with intestinal cancer. (*A*) *IL33* expression in adjacent normal (Norm) colon mucosa and adenomas (Ad). Data obtained from the Sabates-Bellver Colon Oncomine dataset. Bars indicate the mean. (*B*) Serum levels of IL-33 were assessed in healthy individuals ($n = 10$) and CRC patients ($n = 60$) ± SEM by ELISA ($^{\dagger}P \leq 0.01$).

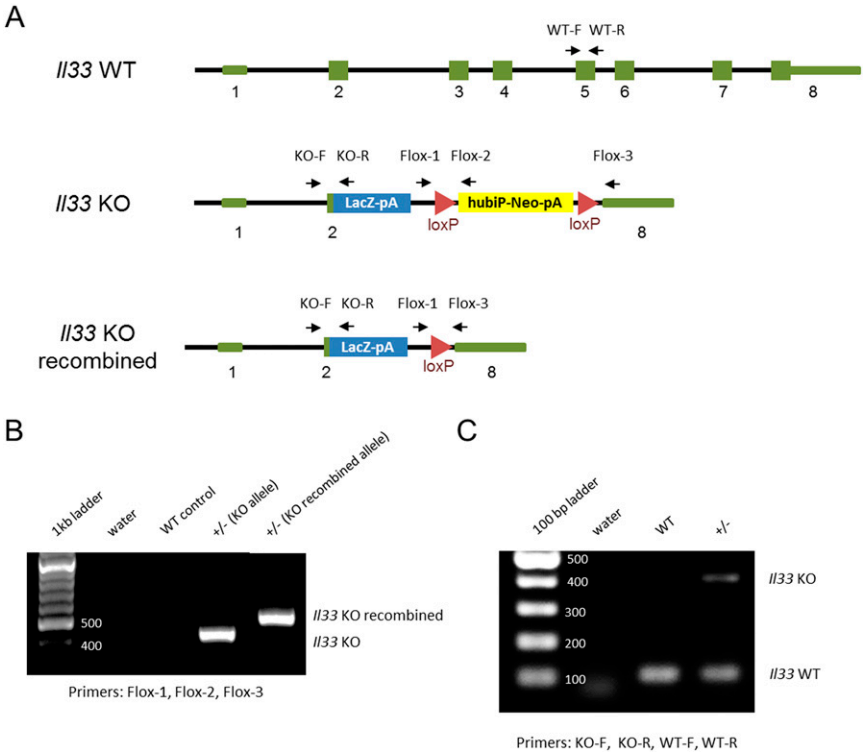

Fig. S2. Engineered deletion of murine *Il33*. (*A*) Genomic structure of the WT and targeted (KO) and Cre recombinase-loxP recombined (KO recombined) *Il33* alleles. The LacZ reporter cassette is inserted immediately downstream and in frame with the translational start site of IL-33 and contains its own stop codon. Thus, no protein coding elements of IL-33 are expressed from the allele. All studies of *Il33*-deficient mice used the KO recombined allele. Locations of PCR primers used for genotyping are indicated. (*B*) PCR genotyping verifying Cre-mediated excision of the Neo cassette. (*C*) PCR genotyping results for the WT and KO recombined allele.

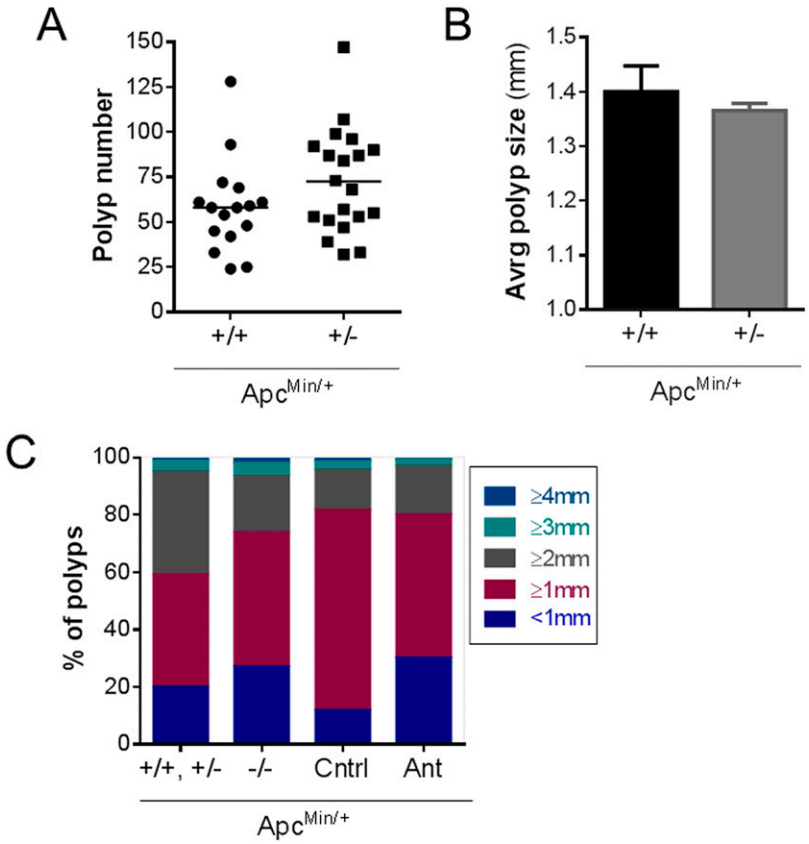

Fig. S3. IL-33 deficiency and polyposis. (*A*) Polyp numbers in 90-d-old $Apc^{Min/+}$ mice WT ($^{+/+}$) or deficient ($^{-/-}$) for *Il33* are statistically similar. Bars indicate the mean. (*B*) Polyp size in $Apc^{Min/+}$ mice WT ($^{+/+}$) or deficient ($^{-/-}$) for *Il33* is statistically similar (±SEM). (*C*) Percent of total polyp number for each size category in $Apc^{Min/+}$ mice WT and heterozygous for the *Il33* deletion ($^{+/+}$ and $^{+/-}$), homozygous for the *Il33* deletion ($^{-/-}$), and treated with a control (Cntrl) or an *Il1rl1* antagonist antibody (Ant).

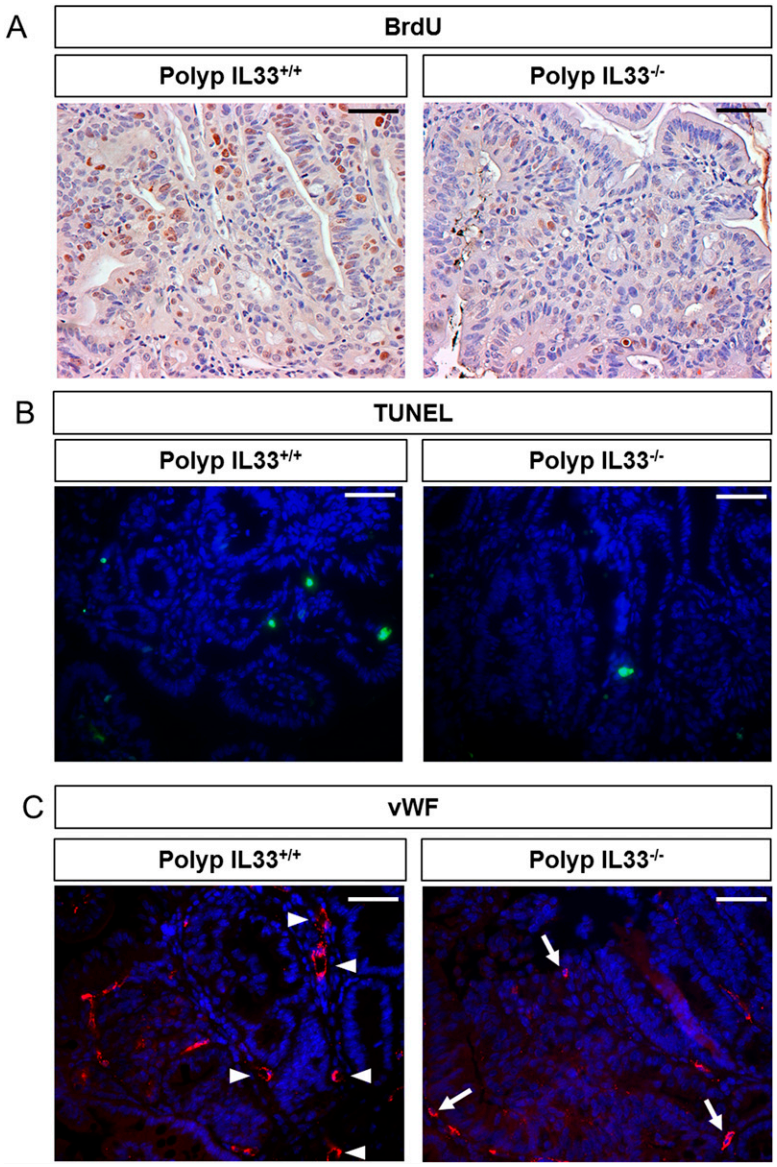

Fig. S4. Representative BrdU, TUNEL, and vWF staining of polyps. (*A*) Bright field microscopy images of polyp sections from *Il33* WT ($^{+/+}$) and deficient ($^{-/-}$) $Apc^{Min/+}$ mice immunolabeled for BrdU incorporation. (*B*) Fluorescent microscopy images of polyp sections from *Il33* WT and *Il33*-deficient $Apc^{Min/+}$ mice labeled by TUNEL assay (blue, DAPI; green, TUNEL-positive). (*C*) Fluorescent microscopy images of polyp sections from *Il33* WT and -deficient $Apc^{Min/+}$ mice immunolabeled for vWF (blue, DAPI; red, vWF). Arrowheads point to endothelial cells forming blood vessels; arrows point to individual cells. For *B* and *C*, nuclei are counterstained with DAPI. (Scale bars, 50 μm.)

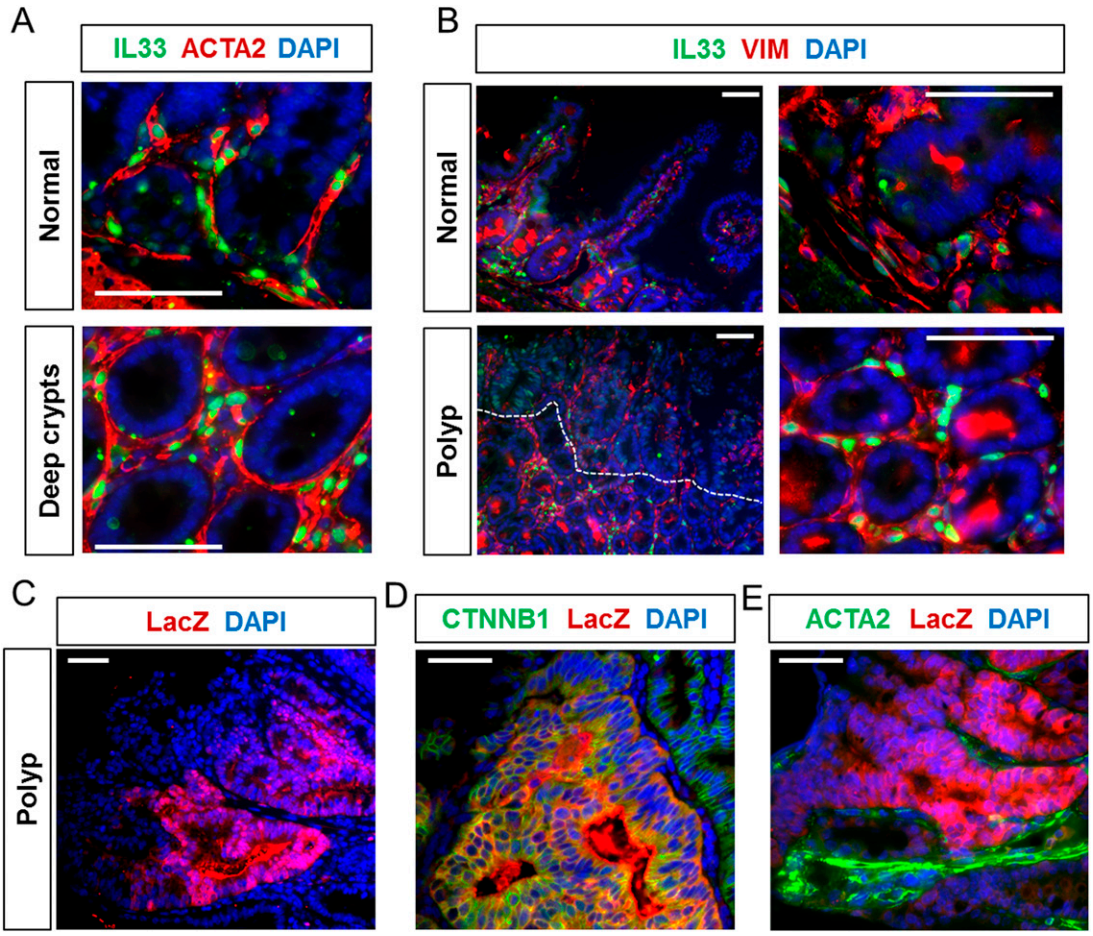

Fig. S5. SEMFs in normal tissue but not polyps express IL-33. (*A*) High-magnification images of sections shown in Fig. 3. IL-33 (green) is expressed by ACTA2-positive (red) SEMFs in normal WT mucosa and in deep crypts under polyp lesions. (*B*) Colocalization of IL-33 (green) and the SEMF marker VIM (red) in cells of WT mucosa and cells surrounding deep crypts under polyp lesions (below the dashed line). SEMFs within the differentiated lesion (above the dashed line) are IL-33–negative. *Right* panels are higher magnification images of *Left* panels. (*C*) Expression of the LacZ reporter knock-in (red), (*D*) colabeling for LacZ and CTNNB1 (green), and (*E*) colabeling for LacZ and ACTA2 (green) in IL-33 heterozygous knockout, $Apc^{Min/+}$ polyps. LacZ expression colocalizes with CTNNB1-positive epithelial cells. Nuclei are counterstained with DAPI. (Scale bars, 50 μm.)

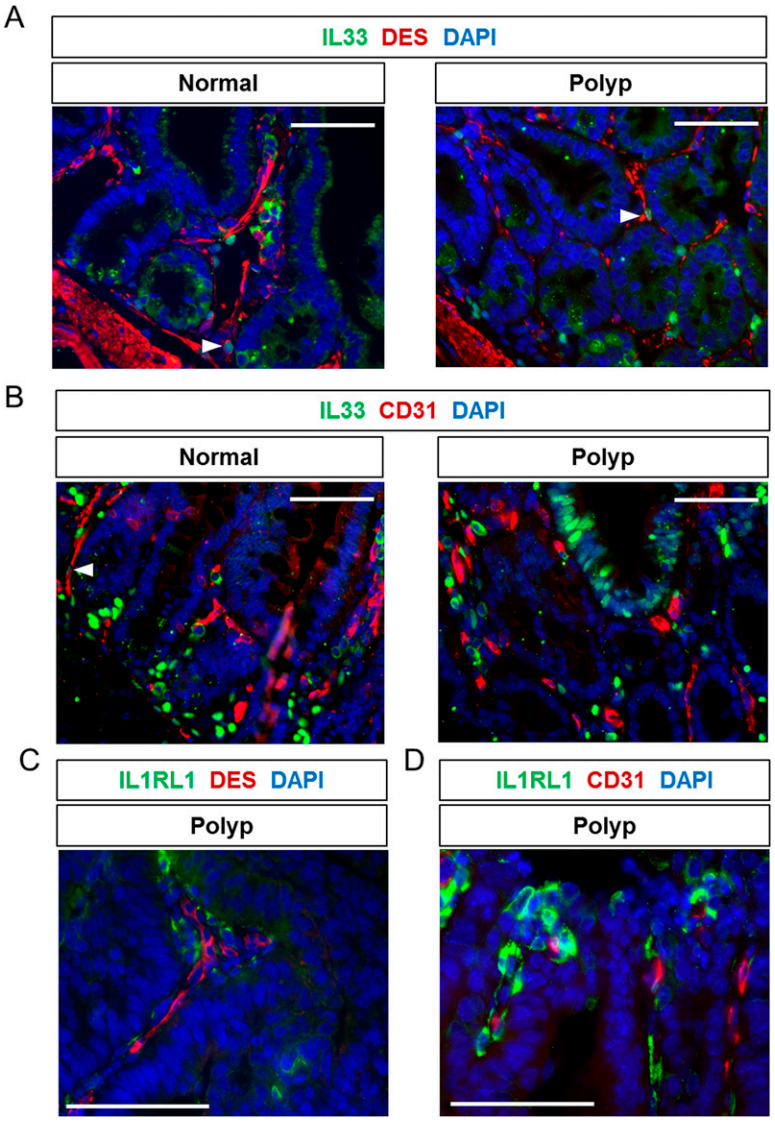

Fig. S6. IL-33 and IL1RL1 expression is rarely detectable in smooth muscle cells or endothelial cells. (*A* and *B*) Immunofluorescence for IL-33 (green) and DES, a marker of smooth muscle cells, or CD31, a marker of endothelial cells (red), in WT (Normal) mucosa and $Apc^{Min/+}$ polyps. Arrowheads indicate rare double-positive cells. Immunofluorescence for IL1RL1 (green) and (*C*) DES or (*D*) CD31 (red) in $Apc^{Min/+}$ polyps. Nuclei are counterstained with DAPI. (Scale bars, 50 μm.)

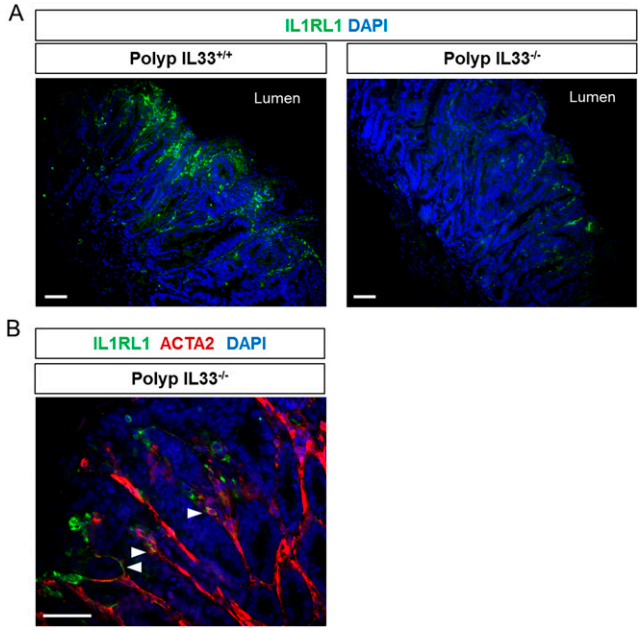

Fig. S7. Expression of IL1RL1 localizes to periluminal cells within the polyp stroma. (*A*) Immunofluorescence for IL1RL1 (green) in polyps of *Il33* WT ($^{+/+}$) and -deficient ($^{-/-}$) $Apc^{Min/+}$ adenomas. Images are oriented with the luminal surface at the top right. (*B*) Immunofluorescence for IL1RL1 (green) and the SEMF marker ACTA2 (red) in a polyp of an *IL33*-deficient $Apc^{Min/+}$ mouse. Nuclei are counterstained with DAPI. White arrowheads indicate double-positive cells. (Scale bars, 50 μm.)

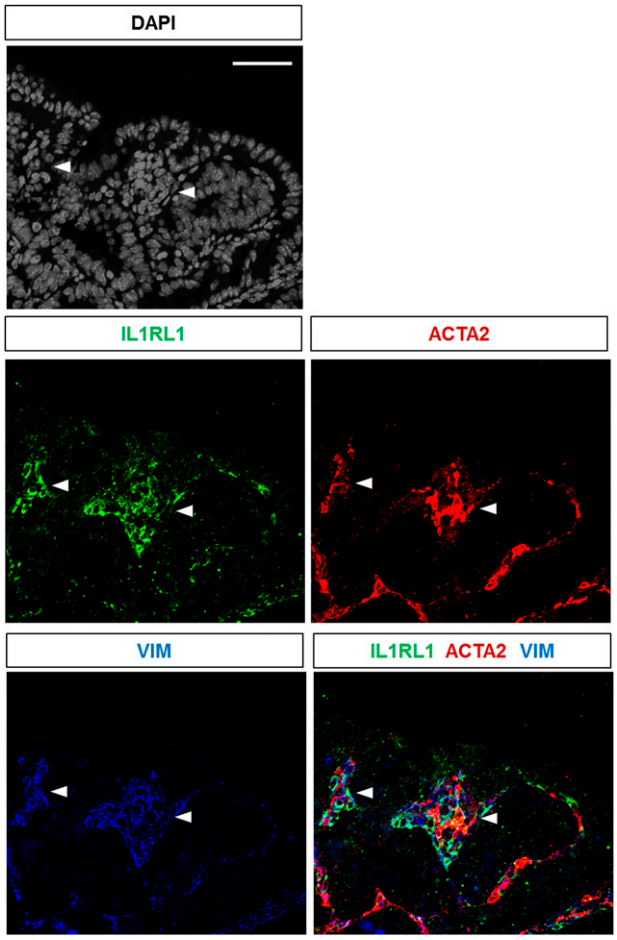

Fig. S8. Colocalization of IL1RL1, ACTA2, and VIM in adenomas. Confocal microscopy images of an $Apc^{Min/+}$ adenoma immunolabeled for IL1RL1, ACTA2, and VIM. Nuclei are counterstained with DAPI. White arrowheads indicate clusters of triple-positive cells. (Scale bars, 50 μm.)

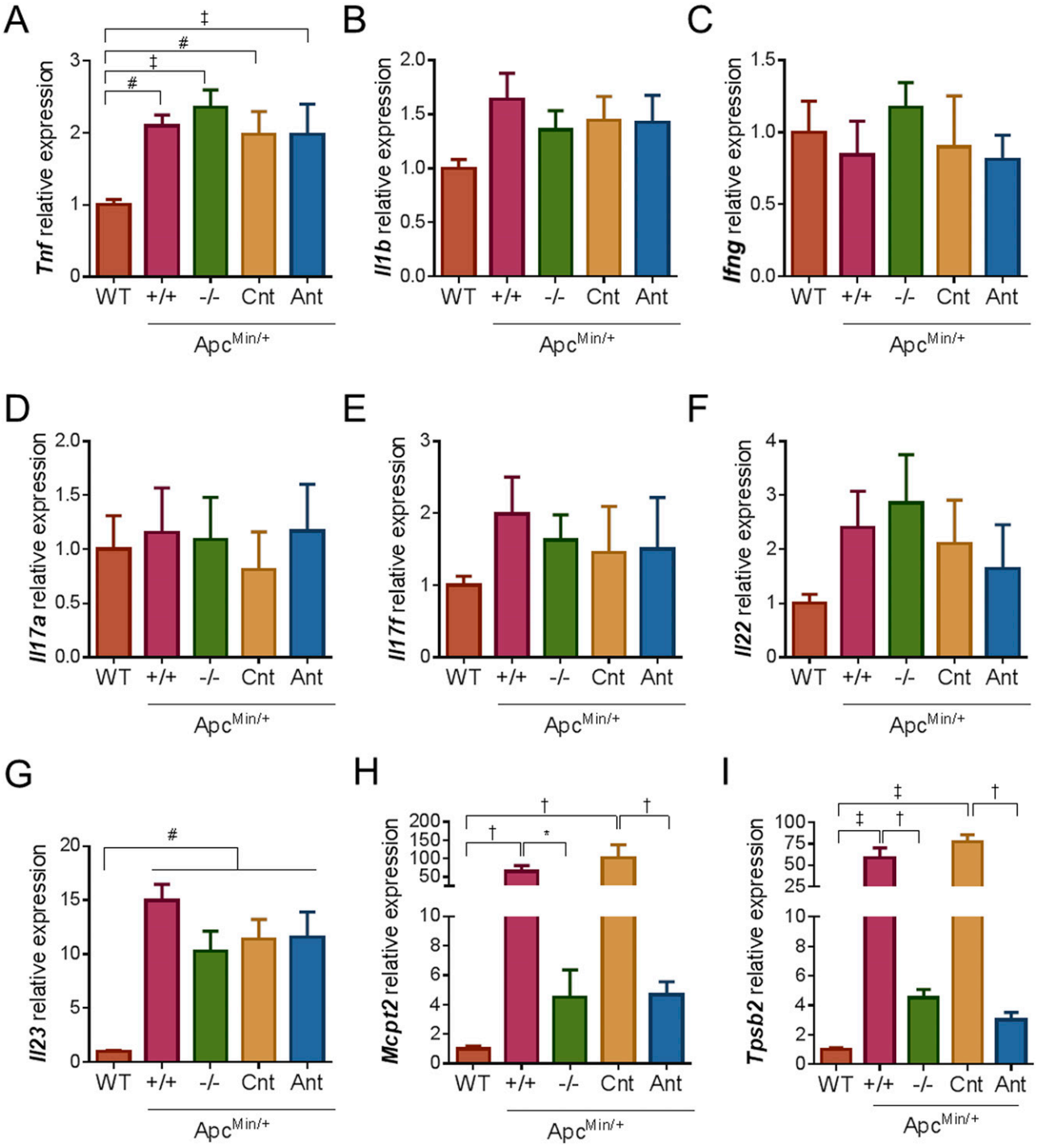

Fig. S9. Expression of inflammatory factors in polyps. qPCR analysis of (*A*) *Tnf*, (*B*) *Il1b*, (*C*) *Ifng*, (*D*) *Il17a*, (*E*) *Il17f*, (*F*) *Il22*, (*G*) *Il23*, (*H*) *Mcpt2*, and (*I*) *Tpsb2* expression in normal mucosa of WT mice, and in adenomas of $Apc^{Min/+}$ ($Apc^{Min/+}$) mice WT ($^{+/+}$) or deficient ($^{-/-}$) for *Il33* or treated with an IgG control antibody (Cnt) or IL1RL1 antagonist antibody (Ant). For all graphs expression is plotted relative to normal mucosa ± SEM (n = 5–10).

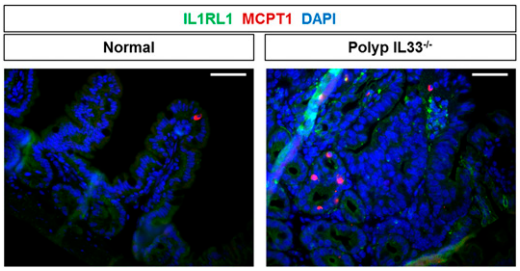

Fig. S10. IL-33 signaling influences mast cell number in polyps. (*A*) Mcpt1-positive (red) mast cells in normal WT mucosa and *Il33*-deficient ($^{-/-}$) $Apc^{Min/+}$ polyps do not express detectable levels of IL1RL1 (green). Nuclei are counterstained with DAPI. (Scale bars, 50 μm.)

Table S1. Sources and working dilutions for primary antibodies

Antibody	Catalog number and source	Working dilution
Goat anti–IL-33 (mouse)	AF3626, R&D Systems	1:20
Goat anti-IL1RL1 (mouse)	AF1004, R&D Systems	1:200
Goat anti–IL-33 (human)	AF3625, R&D Systems	1:50
Rabbit anti-IL1RL1 (human)	11920–1-AP, Proteintech	1:300
Rabbit anti-CTNNB1	ab32572, Abcam	1:300
Mouse anti-ACTA2	ab7817, Abcam	1:50
Chicken anti-VIM	AB5733, Millipore	1:500
Rabbit anti-DES	ab32362, Abcam	1:100
Rabbit anti-CD31	ab28364, Abcam	1:50
Mouse anti-mast cell tryptases	ab2378, Abcam	1:2,000
Rat anti-MCPT1	14–5503, eBiosciences	1:200
Rabbit anti-vWF	A008229, Dako	1:50
Chicken anti–β-galactocidase (LacZ)	ab9361, Abcam	1:1,000

Dataset S1. Cuffdiff differential expression results comparing IL-33–treated and untreated human SEMFs (>1.5-fold change, $P < 0.05$)

Dataset S1

Dataset S2. GO BP and KEGG categories enriched by genes increased >1.5-fold in human SEMFs following IL-33 treatment

Dataset S2

Dataset S3. GO BP and KEGG categories enriched by genes decreased >1.5-fold in human SEMFs following IL-33 treatment

Dataset S3